

Supporting Methods

Metal phthalocyanine $\text{Co}[\text{Pc}(\text{COOH})_4]$ was synthesized on the basis of previous reports.¹ All other reagents and solvents were purchased from commercial sources and used as received.

Synthesis of MOF-74-III spherulite. $\text{Zn}(\text{NO}_3)_2 \cdot 6\text{H}_2\text{O}$ (40 mg), Linker III (15 mg), EtOH (0.1 mL), H_2O (0.1 mL) and DMF (2 mL) were charged into a Pyrex vial. The mixture was heated in 100 °C oven for 24 h. After cooling down to room temperature, the colorless MOF-74-III spherulites were harvested. To better visualize the morphologies of the superstructure, a small amount of dye ligand, metal phthalocyanine $\text{Co}[\text{Pc}(\text{COOH})_4]$, was doped during the one-pot synthesis. $\text{Zn}(\text{NO}_3)_2 \cdot 6\text{H}_2\text{O}$ (40 mg), Linker III (15 mg), CoPc (1 mg), EtOH (0.1 mL), H_2O (0.1 mL) and DMF (2 mL) were charged into a Pyrex vial. The mixture was heated in 100 °C oven for 24 h. After cooling down to room temperature, deep-blue $\text{CoPc}@$ MOF-74-III(Zn) spherulites were harvested. The small amount of deep-blue dye molecules could decorate the superstructures without interrupting the growth of spherulites. These spherulites are then be utilized as seeds for the secondary growth of various MOF-74 isorecticular structures.

Synthesis of MOF-74-II spherulite. $\text{Zn}(\text{NO}_3)_2 \cdot 6\text{H}_2\text{O}$ (40 mg), Linker II (15 mg), EtOH (0.1 mL), H_2O (0.1 mL) and DMF (2 mL) were charged into a Pyrex vial. The mixture was heated in 100 °C oven for 24 h. After cooling down to room temperature, the colorless MOF-74-II spherulites were harvested.

Synthesis of MOF-74-I. $\text{Zn}(\text{NO}_3)_2 \cdot 6\text{H}_2\text{O}$ (40 mg), Linker I (12 mg), EtOH (0.1 mL), H_2O (0.1 mL) and DMF (2 mL) were charged into a Pyrex vial. The mixture was heated in 100 °C oven for 24 h. After cooling down to room temperature, the yellow MOF-74-I were harvested.

Epitaxial growth of MOF-74-III outside MOF-74-III spherulite seeds. MOF-74-III spherulites (5 mg), $\text{Zn}(\text{NO}_3)_2 \cdot 6\text{H}_2\text{O}$ (40 mg), Linker III (15 mg), EtOH (0.1 mL), H_2O (0.1 mL) and DMF (2 mL) were charged into a Pyrex vial. The mixture was heated in 100 °C oven for 24 h. After cooling down to room temperature, the core-shell MOF-

74-III@MOF-74-III was obtained.

Evolution of hierarchical MOF-74-III/plumose MOF-74-II quaternary superstructures. MOF-74-III spherulites (5 mg), $\text{Zn}(\text{NO}_3)_2 \cdot 6\text{H}_2\text{O}$ (40 mg), Linker II (15 mg), EtOH (0.1 mL), H_2O (0.1 mL) and DMF (2 mL) were charged into a Pyrex vial. The mixture was heated in 100 °C oven for 24 h. After cooling down to room temperature, the hierarchical MOF-74-III/plumose MOF-74-II quaternary superstructures were obtained.

Templated evolution of MOF-74-I hollow aggregates. MOF-74-III spherulites (5 mg), $\text{Zn}(\text{NO}_3)_2 \cdot 6\text{H}_2\text{O}$ (40 mg), Linker I (15 mg), EtOH (0.1 mL), H_2O (0.1 mL) and DMF (2 mL) were charged into a Pyrex vial. The mixture was heated in 100 °C oven for 24 h. After cooling down to room temperature, the spherical MOF-74-I particles were obtained.

Powder X-ray diffraction (PXRD). PXRD was carried out with a Bruker D8-Focus Bragg-Brentano X-ray Powder Diffractometer equipped with a Cu sealed tube ($\lambda = 1.54178 \text{ \AA}$) at 40 kV and 40 mA.

^1H NMR spectroscopy. Nuclear magnetic resonance (NMR) data were collected on an Inova 500 spectrometer.

Scanning electron microscopy (SEM). Images and analyses of SEM/EDX were taken by FEI Quanta 600 FE-SEM. The Quanta 600 FEG is a field emission scanning electron microscope capable of generating and collecting high-resolution and low-vacuum images. It is equipped with a motorized x-y-z-tilt-rotate stage, providing the following movements: x = y = 150 mm (motorized); z = 65 mm (motorized); Tilt +70 degrees to -5 degrees (motorized); Source: Field emission gun assembly with Schottky emitter source. Voltage: 200 V to 30 kV. Beam Current: >100 nA.

Supporting Figures

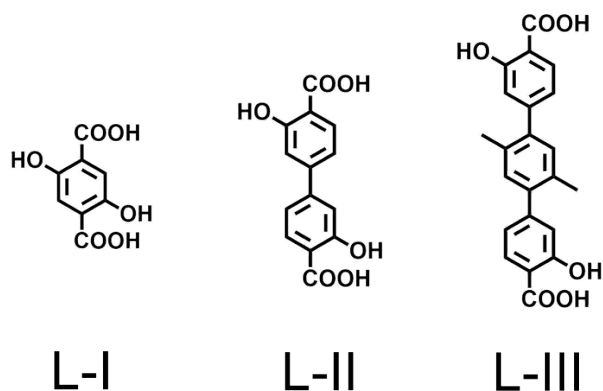


Figure S1. Organic linkers (I-III) used in this study.

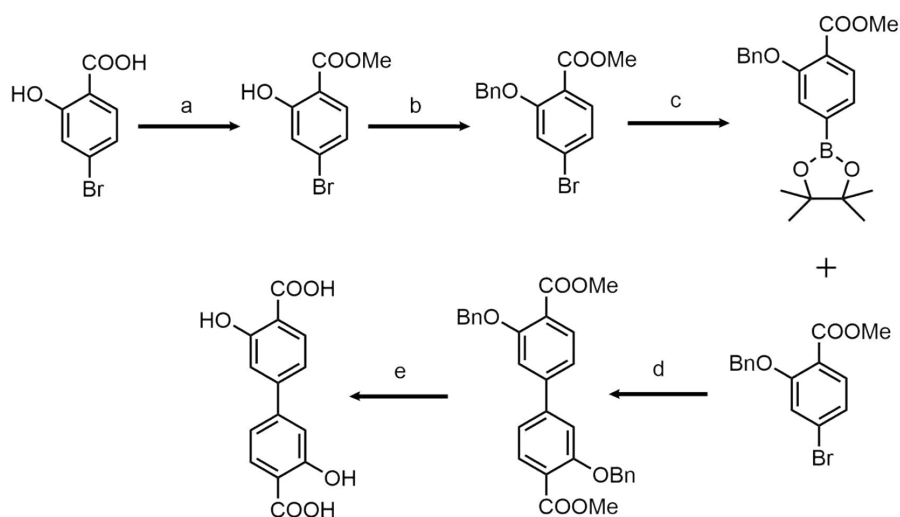


Figure S2. Synthesis of Linker II. a) SOCl₂, MeOH, 75 °C. b) Na₂CO₃, BnBr, MeCN, 75 °C. c) (Bpin)₂, KOAc, Pd(dppf)Cl₂, 85 °C. d) CsF, Pd(dppf)Cl₂, *p*-dioxane/H₂O, 85 °C. e) Pd/C, H₂, THF/MeOH, 50 °C; NaOH, H₂O/THF/MeOH, 85 °C. The synthesis of Linker II was conducted based on previously reported methods.²

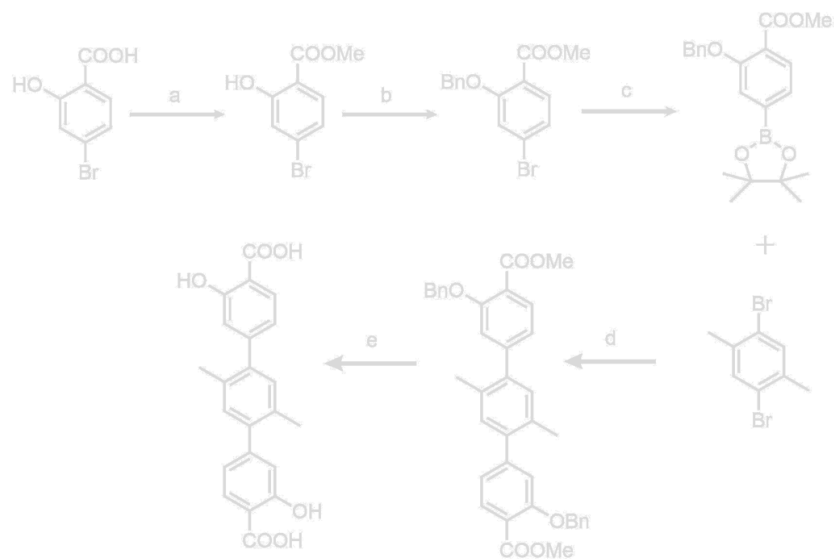


Figure S3. Synthesis of Linker III. a) SOCl_2 , MeOH, 75 °C. b) Na_2CO_3 , BnBr, MeCN, 75 °C. c) $(\text{Bpin})_2$, KOAc, $\text{Pd}(\text{dppf})\text{Cl}_2$, 85 °C. d) CsF, $\text{Pd}(\text{dppf})\text{Cl}_2$, *p*-dioxane/ H_2O , 85 °C. e) Pd/C, H_2 , THF/MeOH, 50 °C; NaOH, H_2O /THF/MeOH, 85 °C. The synthesis of Linker III was conducted based on previously reported methods.²

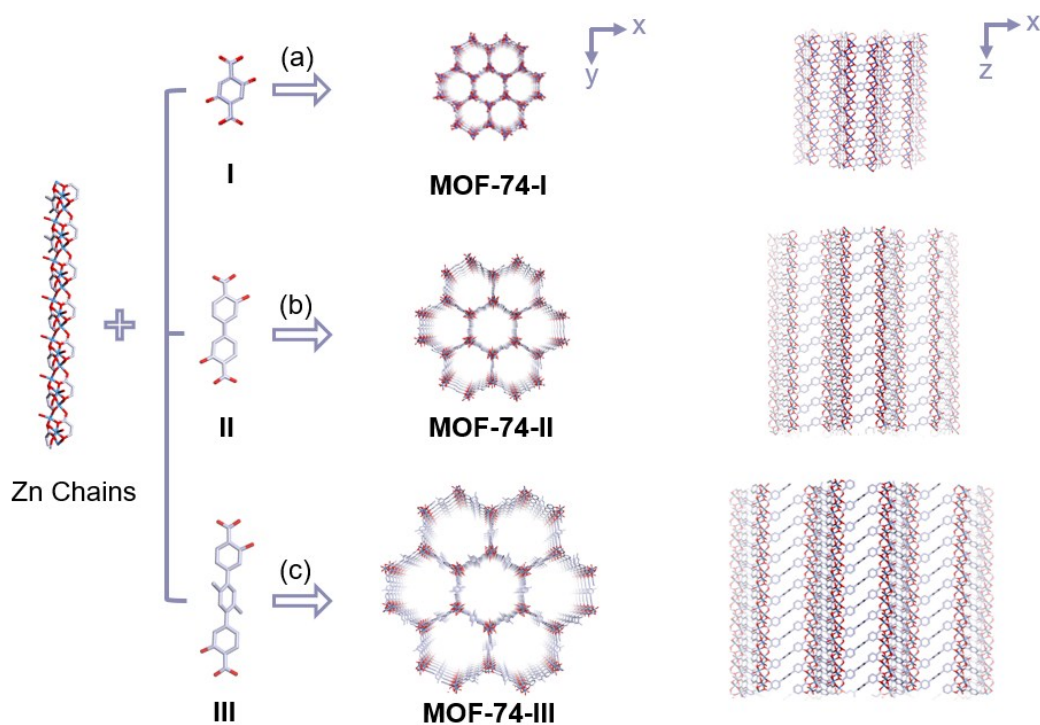


Figure S4. Structure of isoreticular MOF-74-II(Zn) with tunable hexagonal channel sizes: (a) MOF-74-I; (b) MOF-74-II; (c) MOF-74-III.

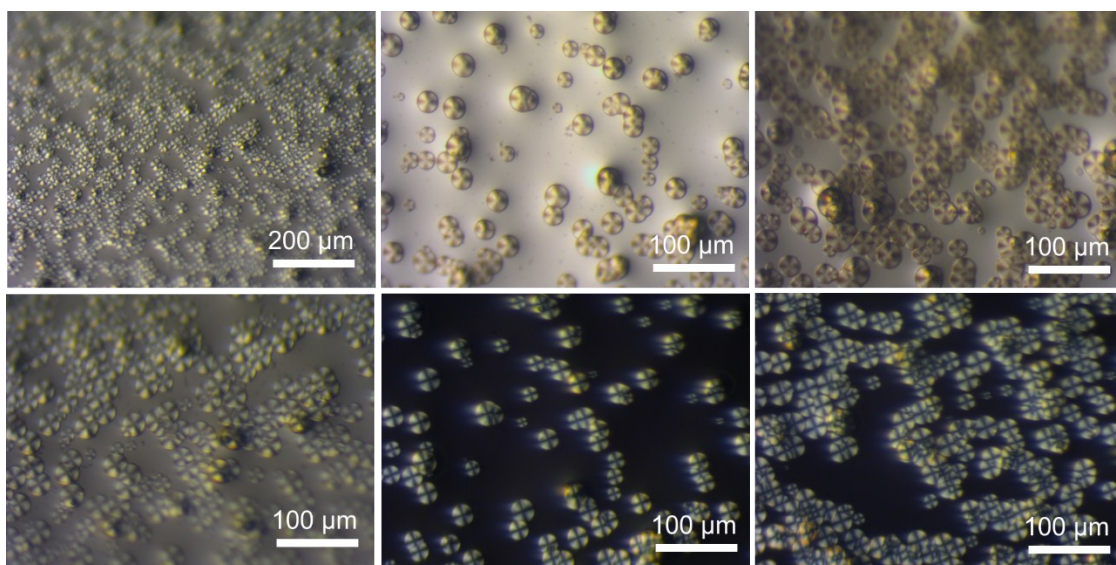


Figure S5. Optical images and corresponding polarized optical images of MOF-74-III spherulite seeds at different scales.

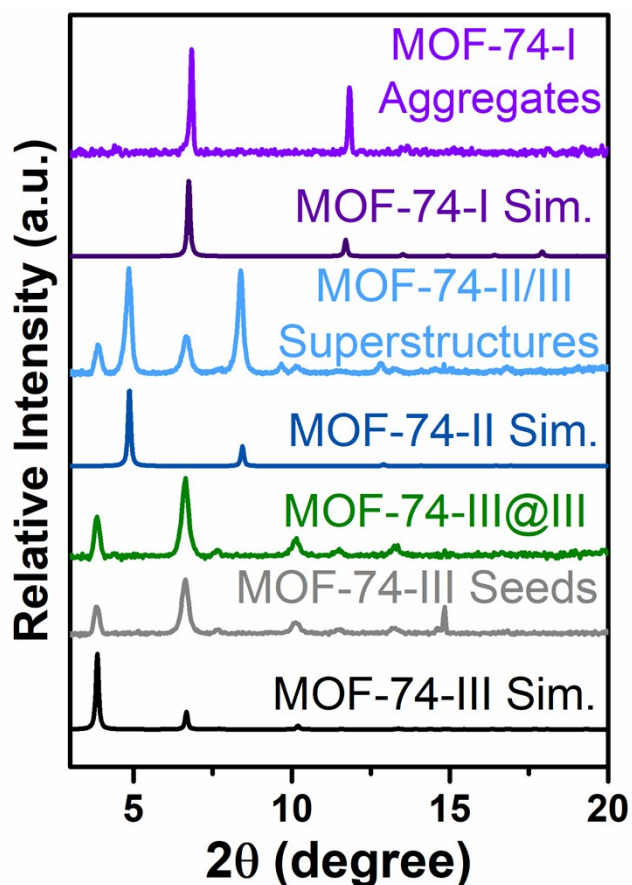


Figure S6. Powder X-ray diffraction (PXRD) patterns of MOF-74-III spherulites, MOF-74-III@MOF-74-III spherulites, spherical MOF-74-III/plumose MOF-74-II quaternary superstructures and MOF-74-I hollow aggregates.

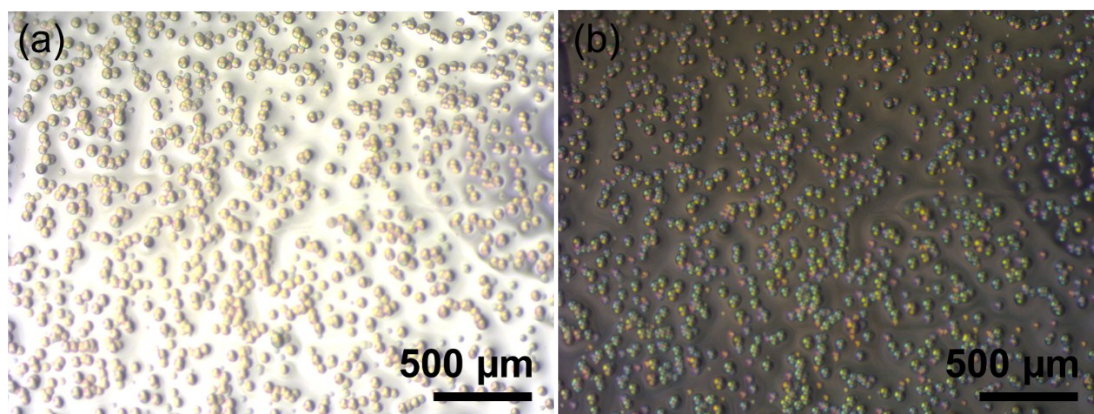


Figure S7. (a) Optical images of MOF-74-II spherulites; (b) Polarized optical image of MOF-74-II spherulites placed in between crossed polarizers.

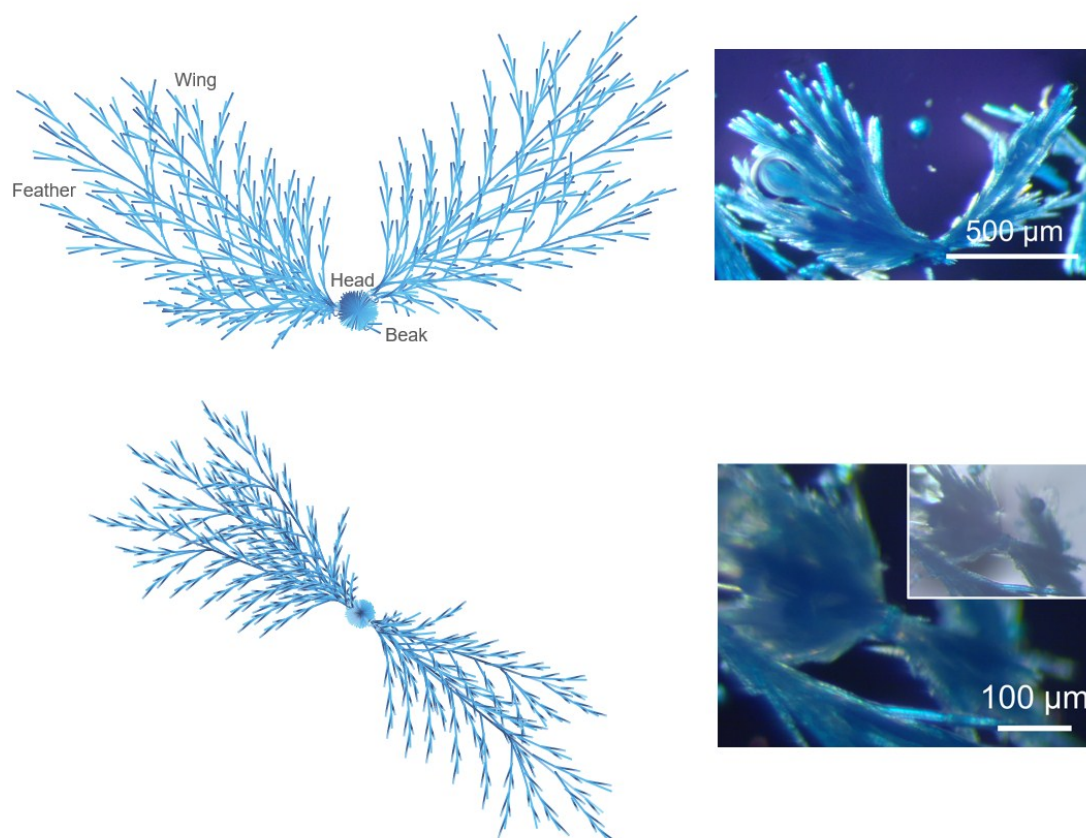


Figure S8. Scheme illustration of the formation of spherical MOF-74-III/plumose MOF-74-II quaternary superstructures, the corresponding optical images and polarized optical images of MOF-74-III/plumose MOF-74-II superstructures. The blue color of the crystals is visualized by the doped dye, metal phthalocyanine ligand.

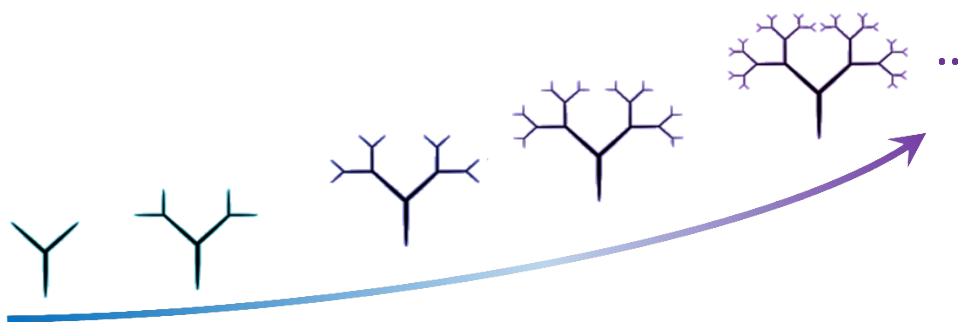


Figure S9. The phenomenon of fractal structures observed both in nature and in this work (plumose MOF-74-II).

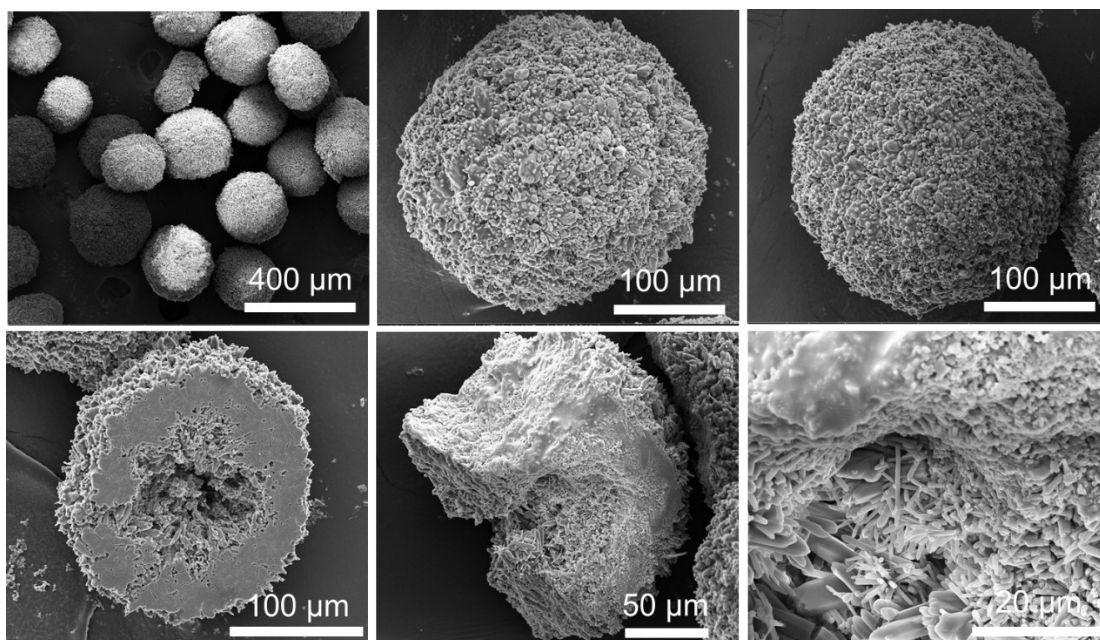


Figure S10. SEM images of hollow sphere aggregates assembled by MOF-74-I needle crystallites.

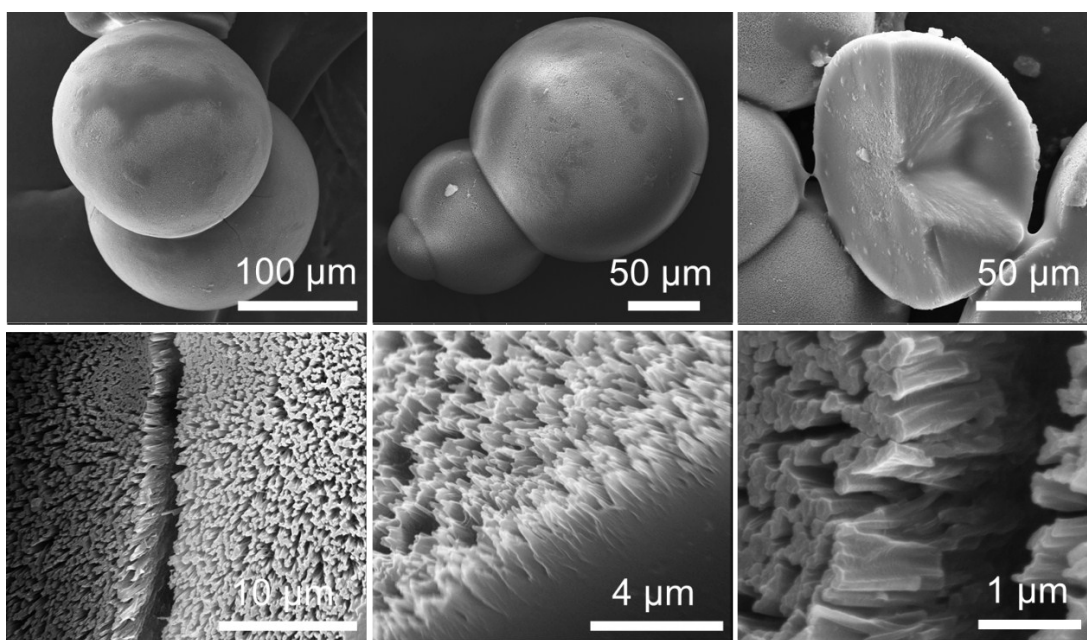


Figure S11. SEM images of MOF-74-III@MOF-74-III spherulites after secondary growth.

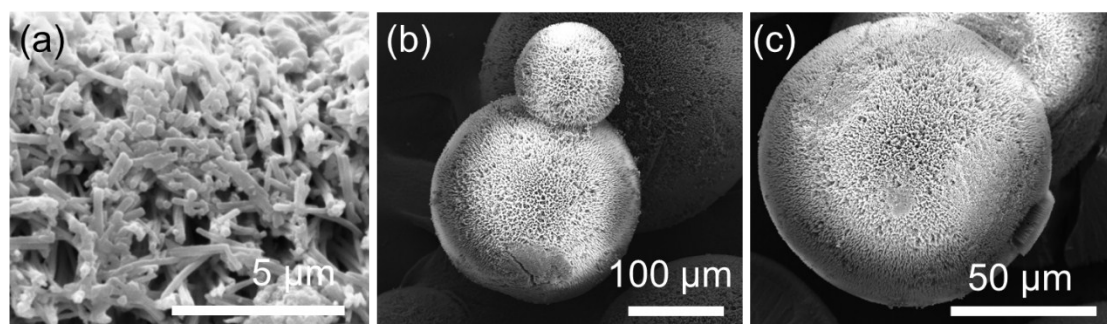


Figure S12. SEM images of pure (a) MOF-74-I needles, (b) MOF-74-II spherulites and (c) MOF-74-III spherulites.

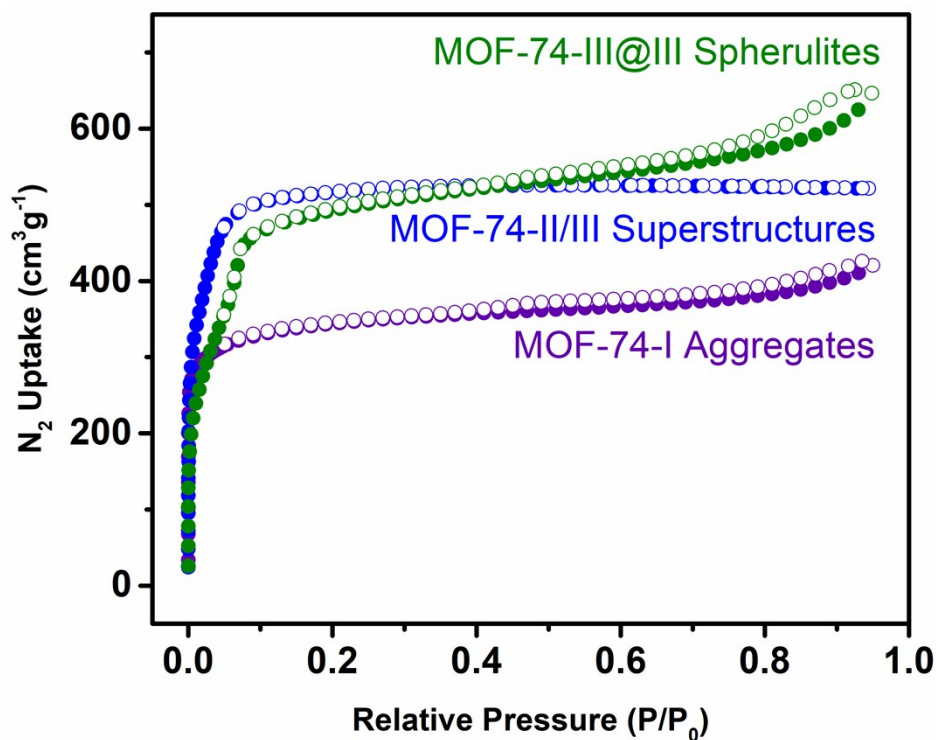


Figure S13. N₂ adsorption isotherms of MOF-74-III@III spherulites, spherical MOF-74-III/plumose MOF-74-II superstructures and MOF-74-I hollow aggregates at 77 K.

References

1. Bai, M.; Song, R.; Zhang, Y.; Han, S.; Song, X.; Meng, F., Trimellitic anhydride- and pyromellitic dianhydride-originated tetrakis/octakis(octyloxycarbonyl)phthalocyaninato metal complexes. *Inorg. Chem. Comm.* **2013**, *28*, 99-103.
2. Peng, S.; Bie, B. L.; Sun, Y. Z. S.; Liu, M.; Cong, H. J.; Zhou, W. T.; Xia, Y. C.; Tang, H.; Deng, H. X.; Zhou, X., Metal-organic frameworks for precise inclusion of single-stranded DNA and transfection in immune cells. *Nat. Commun.* **2018**, *9*, 1293.